

Nonstationary signal inversion based on shaping regularization for random noise attenuation*

Yang Wu-Yang¹, Wang Wei^{*1}, Li Guo-Fa^{2,3}, Wei Xin-Jian¹, Wang Wan-Li¹, and Chen De-wu¹

Abstract: Prediction filtering is one of the most commonly used random noise attenuation methods in the industry; however, it has two drawbacks. First, it assumes that the seismic signals are piecewise stationary and linear. However, the seismic signal exhibits nonstationary due to the complexity of the underground structure. Second, the method predicts noise from seismic data by convolving with a prediction error filter (PEF), which applies inconsistent noise models before and after denoising. Therefore, the assumptions and model inconsistencies weaken conventional prediction filtering's performance in noise attenuation and signal preservation. In this paper, we propose a nonstationary signal inversion based on shaping regularization for random noise attenuation. The main idea of the method is to use the nonstationary prediction operator (NPO) to describe the complex structure and obtain seismic signals using nonstationary signal inversion instead of convolution. Different from the convolutional predicting filtering, the proposed method uses NPO as the regularization constraint to directly invert the effective signal from the noisy seismic data. The NPO varies in time and space, enabling the inversion system to describe complex (nonstationary and nonlinear) underground geological structures in detail. Processing synthetic and field data results demonstrate that the method effectively suppresses random noise and preserves seismic reflection signals for nonstationary seismic data.

Keywords: noise attenuation, nonstationary, inversion, shaping regularization

Introduction

Noise can cause serious confusion over the reflection of seismic signals from actual underground structures. Spatial predictability is the essential difference between seismic signals and random noise (Bednar, 1983; Jones and Levy, 1987; Yu et al., 1989). Thus, various methods have been developed for random noise attenuation (Alan and Panos, 1990; Zhang and Ulrych, 2003;

Neelamani et al., 2008; Gholami, 2014; Wang and Chen, 2019; Zhao et al., 2020). Among these, the most commonly used are prediction filtering in the f-x domain (Canales, 1984; Gulunay, 1986; Chase, 1992; Sun and Ronen, 1996) and t-x domain (Claerbout, 1992; Abma and Claerbout, 1995). However, prediction filtering assumes two inconsistent noise models before and after denoising; thus, it cannot accurately predict the signal (Soubaras, 1994; Zhao et al., 2017). To overcome this model inconsistency, Soubaras (1994, 2000) proposed

Manuscript received by the Editor November 11, 2019; revised manuscript received July 11, 2020.

1. Research Institute of Petroleum Exploration & Development-Northwest, PetroChina, Lanzhou 730020, China.
2. State Key Laboratory of Petroleum Resources and Prospecting, CUP (Beijing), Beijing 102249, China.
3. CNPC Key Laboratory of Geophysical Prospecting, CUP (Beijing), Beijing 102249, China.

♦Corresponding author: Wang Wei (Email: ww_geophy@126.com).

© 2020 The Editorial Department of **APPLIED GEOPHYSICS**. All rights reserved.

projection filtering for random noise attenuation, which enhances the recovery of seismic signals. Prediction filtering based on the autoregressive–moving average model (Sacchi and Kuehl, 2001; Liu et al., 2009) can also achieve a denoising effect similar to that of projection filtering. The difference is that prediction filtering estimates the filter by solving the eigenvalue problem, while projection filtering obtains the filter by iterative calculation.

The strategy of a short temporal window is the simplest noise attenuation method for nonstationary seismic signals (Crawley et al., 1999). However, this strategy is difficult to adapt to processing complex nonstationary seismic signals. Fomel (2007, 2009) proposed regularized nonstationary regression (RNR) for shaping regularization; in this approach, the operator for predicting the spatiotemporal variation of the signal is obtained by solving the global minimization problem. Thus, it can be adapted to nonstationary seismic signals that vary with time and space. Liu and Fomel (2010) employed RNR to calculate adaptive prediction-error filters (PEFs) in the t-x domain for trace interpolation. Liu et al. (2012, 2013) applied RNR in the f-x domain and f-x-y domain for random noise attenuation, which can be adapted to predicting nonstationary signals that vary in dip or amplitude. Liu et al. (2014) proposed adaptive prediction filtering in the t-x-y domain for random noise attenuation based on RNR.

In addition to denoising, a filter should also be able to preserve the signal. Yuan et al. (2012) proposed an edge-preserving random noise attenuation method based on inversion. The denoised seismic data were taken as model parameters, and the total variation (TV) model (Rudin et al., 1992) was used as a regularization constraint to directly invert the seismic signal from noisy seismic data. However, the TV model cannot adaptively describe complex structures. To overcome this problem, Zhao et al. (2017) introduced PEF as a regularization constraint to prediction filtering and proposed an inversion-based data-driven method for random noise attenuation in the t-x domain. While Yuan et al.'s (2012) method uses a model-driven algorithm, Zhao et al.'s (2017) method calculates the regularization constraint from the seismic data itself; thus, it is a data-driven algorithm with stronger denoising ability. However, the assumptions of prediction filtering limit the prediction ability of Zhao et al.'s method when the underground structure is very complex because a stationary PEF is used as a regularization constraint, and seismic signals are assumed to be piecewise stationary and linear.

Based on the data-driven seismic signal inversion proposed by Zhao et al. (2017), in this paper we propose a

random noise attenuation method for the inversion of nonstationary signals by shaping regularization. Our method uses shaping regularization to calculate the operator for predicting a signal that varies with time and space, and it does not assume a piecewise stationary and linear signal. Thus, it can be used to characterize complex geologic structures. The proposed method was applied to a series of models and real data from an oil field in eastern China, and the results were used to verify its effectiveness at noise attenuation and signal preservation for nonstationary data.

Theory

Prediction filtering in t-x domain

According to the prediction filtering, the linear and stationary seismic signal in a trace can be predicted by the adjacent seismic trace owing to its spatial predictability (Canales, 1984); thus, the seismic signal s can be written as:

$$s(ix, it) = \sum_{jx=-mx, jx \neq 0}^{mx} \sum_{jt=-mt}^{mt} f(jx, jt)s(ix - jx, it - jt), \quad (1)$$

where f is PF, ix and jx are spatial indices, it and jt are temporal indices, mx and mt are the length of t-x domain PF in the space and time directions, respectively. The form of PF with $mx = 2$ and $mt = 2$ is:

$$\begin{matrix} f_{-2,-2} & f_{-1,-2} & 0 & f_{1,-2} & f_{2,-2} \\ f_{-2,-1} & f_{-1,-1} & 0 & f_{1,-1} & f_{2,-1} \\ f_{-2,0} & f_{-1,0} & 0 & f_{1,0} & f_{2,0} \\ f_{-2,1} & f_{-1,1} & 0 & f_{1,1} & f_{2,1} \\ f_{-2,2} & f_{-1,2} & 0 & f_{1,2} & f_{2,2} \end{matrix} \quad (2)$$

We obtain the PF f from noisy data d by solving the following least-squares problem:

$$J = \sum_{ix} \sum_{it} \left\| d(ix, it) - \sum_{jx=-mx, jx \neq 0}^{mx} \sum_{jt=-mt}^{mt} f(jx, jt)d(ix - jx, it - jt) \right\|^2 + \mu \sum_{jx=-mx, jx \neq 0}^{mx} \sum_{jt=-mt}^{mt} \|f(jx, jt)\|^2, \quad (3)$$

where $\|\bullet\|^2$ denotes the square of the l_2 norm and ε is a

Nonstationary signal inversion based on shaping regularization

scalar regularization parameter. We obtain the denoised data d' by calculating 2D convolution of the PF f and noisy data d :

$$d' = f * d. \quad (4)$$

The prediction filtering assumed two inconsistent noise models before and after denoising, which decreased noise attenuation and signal preservation (Soubaras, 1994; Liu et al., 2009, Zhao et al., 2017). On the other hand, the prediction filtering applies the same PF f to all seismic data in the processing window, requiring the assumption that the seismic signals are stationary and the events are linear. However, the real seismic data are mostly nonstationary, and the events are nonlinear. Thus, the stationary PF is difficult to consider all seismic data and accurately describes the geological structure, causing damage to the seismic signal. Aiming at this problem, Liu et al. (2014) proposed an adaptive prediction filtering and calculated the APF using nonstationary autoregression. The APF varies with time and space; thus, it can describe complex underground geological structures.

We obtain the APF coefficients $F_{i,j}(t,x)$ by solving the following least-squares problem. Unlike equation (3), the equation is underdetermined and can be solved using a conjugate-gradient algorithm with shaping regularization (Fomel, 2007).

$$\begin{aligned} \tilde{F}_{i,j} = \arg \min_{F_{i,j}(t,x)} & \left\| d(t,x) - \sum_{j=-N, j \neq 0}^N \sum_{i=-M}^M F_{i,j}(t,x) d_{i,j}(t,x) \right\|^2 \\ & + \mu^2 \sum_{j=-N, j \neq 0}^N \sum_{i=-M}^M \left\| \mathbf{R} [F_{i,j}(t,x)] \right\|^2, \end{aligned} \quad (5)$$

where i and j are temporal and spatial indices for APF, respectively; t and x are temporal and spatial indices for seismic, respectively M and N indicate the size of APF in the time and space directions, respectively; the μ is a scalar regularization parameter and $\mathbf{R}[\bullet]$ indicates shaping regularization, which is implemented by a triangular smoothing filter (Fomel, 2007), whose length is called the smoothing radius. As the smoothing radius of the APF increases, the APF removes more random noise and some structural details.

Similar to the stationary prediction filtering, we can obtain the denoised seismic data S by nonstationary prediction filtering as follows:

$$S(t,x) = \sum_{j=-N, j \neq 0}^N \sum_{i=-M}^M F_{i,j}(t,x) d_{i,j}(t,x). \quad (6)$$

Nonstationary signal inversion for random noise attenuation

Unlike the stationary prediction filtering, which directly convolves the PF with the seismic data to obtain the denoised data, the proposed method uses the NPO as the regularization constraint of the inversion. It regards denoised data as a model parameter in the inversion. We obtain the denoised data by inverting these parameters from the noisy seismic data. The NPO $\bar{\mathbf{F}}(t,x)$ has the same coefficients as the APF $\mathbf{F}(t,x)$, except that the value at the output position is -1, which has the following form if $M = 2$ and $N = 2$:

$$\begin{aligned} & F_{-2,-2}(t,x) \quad F_{-1,-2}(t,x) \quad 0 \quad F_{1,-2}(t,x) \quad F_{2,-2}(t,x) \\ & F_{-2,-1}(t,x) \quad F_{-1,-1}(t,x) \quad 0 \quad F_{1,-1}(t,x) \quad F_{2,-1}(t,x) \\ & F_{-2,0}(t,x) \quad F_{-1,0}(t,x) \quad -1 \quad F_{1,0}(t,x) \quad F_{2,0}(t,x) \\ & F_{-2,1}(t,x) \quad F_{-1,1}(t,x) \quad 0 \quad F_{1,1}(t,x) \quad F_{2,1}(t,x) \\ & F_{-2,2}(t,x) \quad F_{-1,2}(t,x) \quad 0 \quad F_{1,2}(t,x) \quad F_{2,2}(t,x) \end{aligned} \quad (7)$$

As shown in equation (7), the NPO structure excludes the causal time prediction coefficients (i.e., $F_{0,j}(t,x) = 0, j \neq 0$), and forces only lateral predictions.

The objective function of the nonstationary seismic signal inversion can be expressed as:

$$\begin{aligned} \tilde{S}(t,x) = \arg \min_{S_{i,j}(t,x)} & \left\| d(t,x) - S(t,x) \right\|^2 \\ & + \lambda \sum_{j=-N}^N \sum_{i=-M}^M \left\| \bar{\mathbf{F}}_{i,j}(t,x) S_{i,j}(t,x) \right\|_L^k. \end{aligned} \quad (8)$$

For simplicity, we rewrite equation (8) in matrix form as:

$$J = \|\mathbf{d} - \mathbf{S}\|^2 + \lambda \|\mathbf{PS}\|_L^k, \quad (9)$$

where d and S are vectors, $\mathbf{d} = [d(1,1), d(2,1), \dots, d(Nt, Nx)]^T$, and Nt and Nx are noisy data sizes in time and space directions, respectively, \mathbf{S} is the signal or denoised data. λ is a scalar trade-off parameter, L is a norm, k is a power. When $L = 1$ ($k = 1$), the second term is l_1 norm, and when $L = 2$ ($k = 2$), the second term is l_2 norm. \mathbf{P} is a $(Nt \times Nx) \times (Nt \times Nx)$ matrix rearranged by $\mathbf{F}_{i,j}(t,x)$ according to the calculation correspondence.

The first term in equation (9) describes the energy difference between the effective signal and the noisy seismic data, which guarantees this method's signal-

preservation capability. The second term is the regularization term, which describes the seismic signal's predictability and ensures noise attenuation effectiveness. The NPO describes the geological structure. If the inverted signal is laterally discontinuous, then the signal is unpredictable, which leads to the larger value of the second term in equation (9). However, if the inverted signal is laterally continuous and conforms to NPO's geological structure, the signal is predictable, leading to the second term's smaller value. We can get the seismic signal following the geological law by minimizing the objective function. The trade-off parameter λ determines the contribution of the two terms to the objective function and affects noise attenuation performance. If λ is too small, several noise may remain. However, if λ is too large, the effective signal may be damaged. Therefore, we need to choose reasonable parameter λ to achieve a balance between noise attenuation and signal preservation. The second term of equation (9) can select l_1 norm, l_2 norm, or other norms. When $L = 2$, the solution of the objective function 9 is:

$$\mathbf{S} = (\mathbf{I} + \lambda \mathbf{P}^T \mathbf{P})^{-1} \mathbf{d}. \quad (10)$$

To improve the computational efficiency, we obtain the denoised data \mathbf{S} by calculating equation (10) using the conjugate-gradient algorithm instead of matrix operation. The calculation process of the proposed method is as follows:

- 1) Calculate the NPO:

$$\tilde{F}_{i,j} = \arg \min_{F_{i,j}(t,x)} \left\{ \left\| d(t,x) - \sum_{j=-N, j \neq 0}^N \sum_{i=-M}^M F_{i,j}(t,x) d_{i,j}(t,x) \right\|^2 + \varepsilon^2 \sum_{j=-N, j \neq 0}^N \sum_{i=-M}^M \left\| \mathbf{R} [F_{i,j}(t,x)] \right\|^2 \right\}, \quad (11)$$

- 2) Invert signal constrained by the NPO:

$$J = \|\mathbf{d} - \mathbf{S}\|^2 + \lambda \|\mathbf{PS}\|_L^k. \quad (12)$$

Synthetic model test

We design two synthetic seismic models with nonstationary signals to test and analyze the noise suppressing and signal-preserving performance of the

proposed method (NSI). For comparison, we use the RNA (i.e., the f-x domain prediction filtering) in the GeoEast software, the inversion-based t-x domain random noise attenuation method (Zhao et al., 2017, hereinafter referred to as IRNA) and APF (Liu et al., 2014) based on RNA to process the data simultaneously. To quantify the denoising effect of the above four methods, we define the SNR as follows:

$$SNR = 10 \log_{10} \frac{\|\mathbf{S}\|_F^2}{\|\mathbf{D} - \mathbf{S}\|_F^2}, \quad (13)$$

where \mathbf{S} is the true signal, \mathbf{D} is the noisy data, and $\|\bullet\|_F^2$ is the square of Frobenius norm. Figure 1 shows the SNR of the data after denoising with the above four methods.

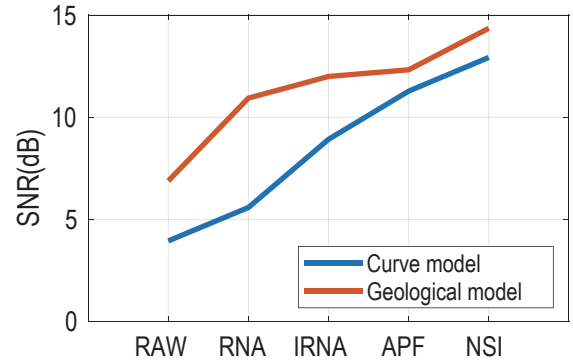


Fig. 1. SNR of data after denoising by the four methods (Unit: dB).

The first model is a curve model. Fig. 2(a) shows the clean synthetic data in which the event's travel-time is a sinusoidal function, and the wavelet is a 30-Hz Ricker wavelet. The model has 100 traces. The amplitude of each trace data is nonstationary, and the maximum amplitude varies with the traces: $A(x) = 2/nx^2(x-nx/2)^2 + 0.5$, where nx is the traces number and x is the traces index. The time length is 200 ms, and the sampling rate is 2ms. We added Gaussian noise to the clean data, as shown in Figure 2a), and obtained the noisy data (see Fig. 2(b)) with $SNR=3.94$ dB. To approximate the real random noise, the added Gaussian noise was low-pass filtered. The RNA implemented with the length of the PF is 7. For IRNA, the PF length in the time and space direction is 10 and 7, respectively ($mt = 10$ and $mx = 7$ in equation (3)); the trade-off parameter is 1. For APF, the length of the filter in the time and space direction are 5 and 2, respectively ($M = 5$ and $N = 2$ in equation (5)); the smoothing radius is 20. For NSI, the NPO's length in the time and space direction are 5 and

Nonstationary signal inversion based on shaping regularization

2, respectively ($M = 5$ and $N = 2$ in equation (8)); the trade-off parameter is 10. Figure 3 shows the denoised results and the removed noise of the three methods. RNA applies inconsistent noise models before and after denoising (Soubaras, 1994; Liu et al., 2009; Zhao et al., 2017) and assumes that the seismic signal is stationary and events are linear (Canales, 1984). Therefore, it is difficult to reduce random noise from nonstationary seismic data (Figure 3)), while it is easy to damage the effective signal (Figure 3b)). IRNA uses inversion to denoise instead of convolution and overcomes the model inconsistencies, removing more random noise than the RNA (Figure 3c). However, its regularization conditions

are derived from conventional PFs and cannot describe complex geological structures; thus, causing damage to effective signals (Figure d). APF uses the nonstationary PF to predict the signal without the assumption of stationary signals and linear events. Therefore, it has some advantages in nonstationary signal preservation. NSI uses the NPO as a regularization constraint inversion to reduce random noise, which requires assumptions and overcomes the model inconsistencies. Therefore, NSI is more effective in noise attenuation and signal preservation for nonstationary data than the other three methods (see Figures 3 (g), (h), and Figure. 1).

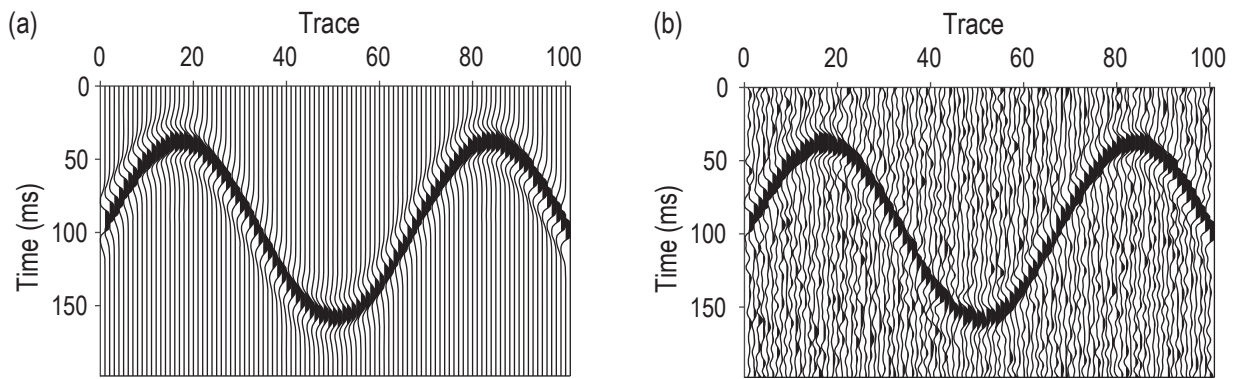
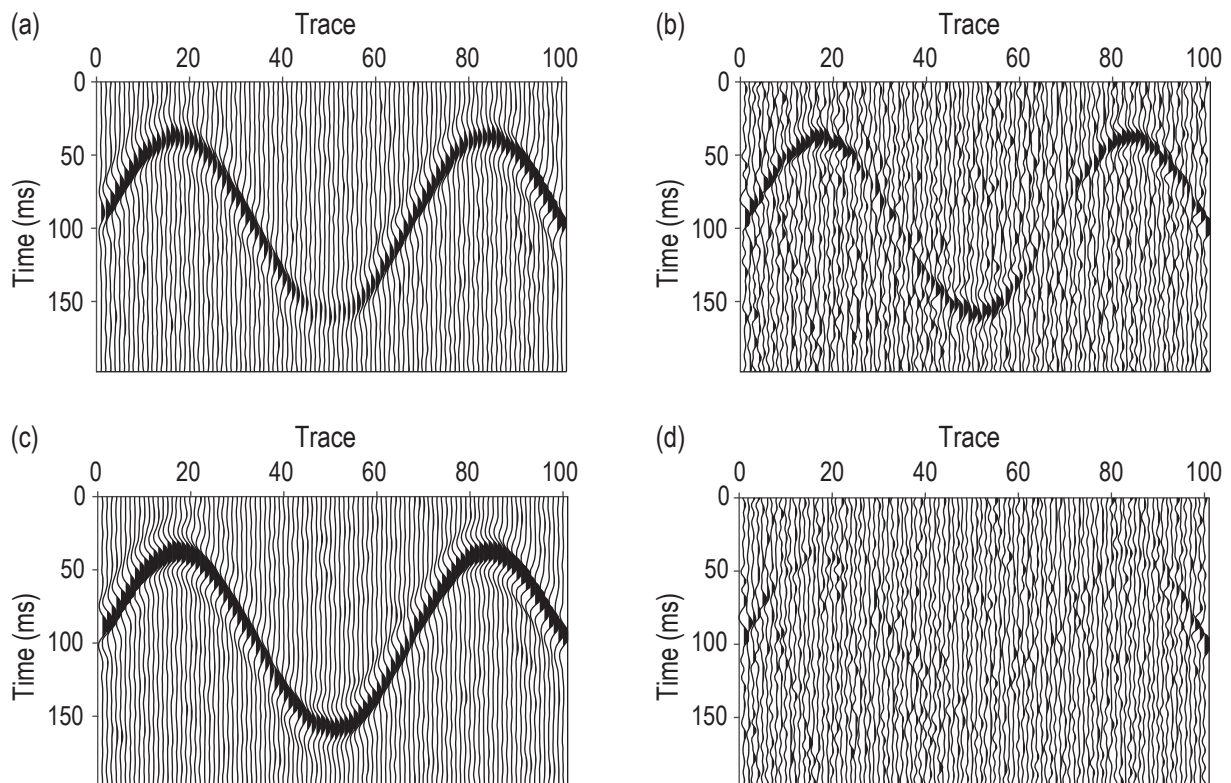


Fig. 2. Curved model (a) clean data, (b) noisy data.



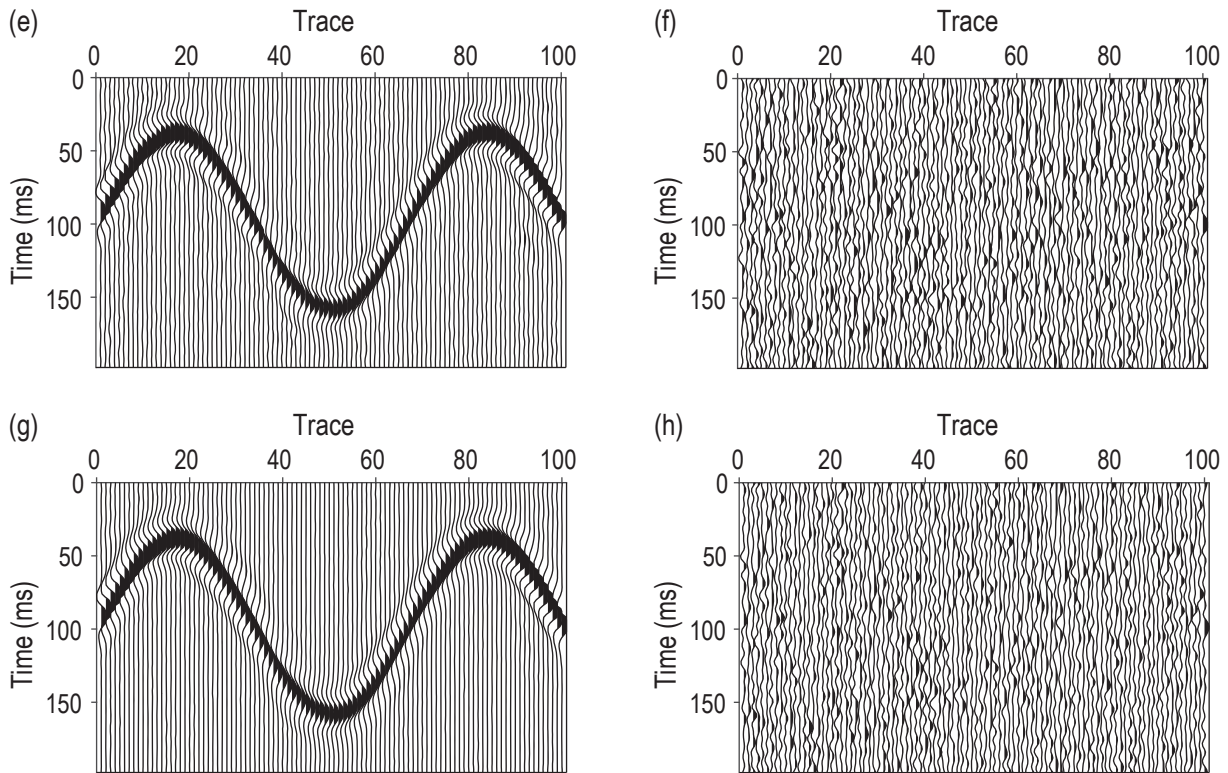


Fig. 3. Comparison of the three methods: (a) the denoised results by RNA (b) the removed noise by RNA (c) the denoised results by IRNA (d) the noise removed by IRNA (e) the denoised results by APF (f) the noise removed by APF (g) the denoised results by NSI (h) the noise removed by NSI.

The second model is a 2D geological model with fold and fault structures. Figure 4 shows the velocity model. The horizontal length is 1600m, and the time depth is 500 ms. The shallow layers of the model are horizontal strata, and the underlying strata are folded structures. The seismic data is synthesized by convoluting Ricker wavelet; whose dominant frequency is 30 Hz. Figure 5a shows that the seismic data has 101 traces and 251 sampling points. The sampling rate is 2ms, and the time length is 500 ms. The fold and fault structures from 150 ms to 350ms are used to investigate the denoising method's effectiveness for nonstationary data. The weak signal around 400ms is used to examine the denoising method's performance in recovering weak signals. Figure 5b shows noisy data with $SNR = 6.88$ dB. To reduce SNR of noisy seismic data at strong amplitude, the energy of simulated random noise is enhanced by equation (14) after low-pass filtering. We applied the above four methods, RNA, IRNA, APF, and NSI, to suppress random noise. The RNA is implemented with the length of the PF is 7. For IRNA, the PF's length in the time and space direction are 31 and 20, respectively

($mt = 15$ and $mx = 10$ in equation (3)); the trade-off parameter is 2. For APF, the length of the filter in the time and space direction are 5 and 3, respectively ($M = 5$ and $N = 3$ in equation (5)), the smoothing radius is 10. For NSI, the NPO's length in the time and space direction are 5 and 3, respectively ($M = 5$ and $N = 3$ in equation (8)), the smoothing radius is 10, and the trade-off parameter is 5. Figure 6 shows the denoised results and the removed noise of the four methods. As shown in Figure 6a, 6c, 6e, 6f, and Figure 1, NSI removes more noise than the other two methods. As for the processing results of the RNA, the signals of the fold and fault structure in the noise section are very obvious, and the weak signal in the denoised data section becomes laterally discontinuous (see Figure 6a), indicating that the RNA is not suitable for nonstationary data. IRNA performs better than RNA in weak signal protection (see Figure 5c); however, it is not suitable for nonstationary data. If the dip and amplitude of the event vary sharply, the method may damage the effective signal (see Figure 6d). APF method is suitable for nonstationary data, and it does not cause obvious damage to the effective signal.

Nonstationary signal inversion based on shaping regularization

Still, the denoising effect is slightly inferior to NSI (see Figure 6e) and Figure 1). For NSI, the noise section's signal is almost invisible (see Figure 6f). The denoised result's weak signal is clear and laterally continuous, and the seismic structure remains complete (Figure 6e).

$$\tilde{\mathbf{N}} = \max\left(1, 2 \times \frac{|\mathbf{S}|}{\max(|\mathbf{S}|)}\right) \odot \mathbf{N}, \quad (14)$$

where, \mathbf{N} is the noise data after low-pass filtering and \odot is Hadamard product.

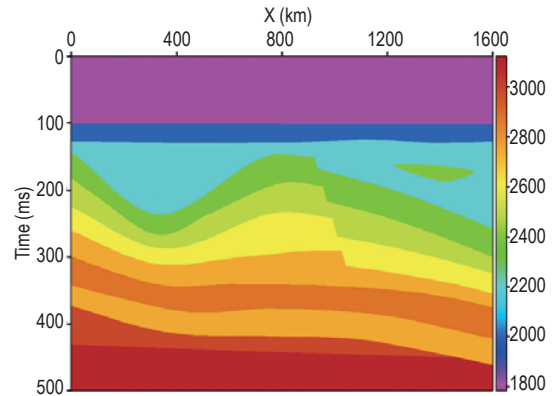


Fig. 4. 2D geological model with folded structures.

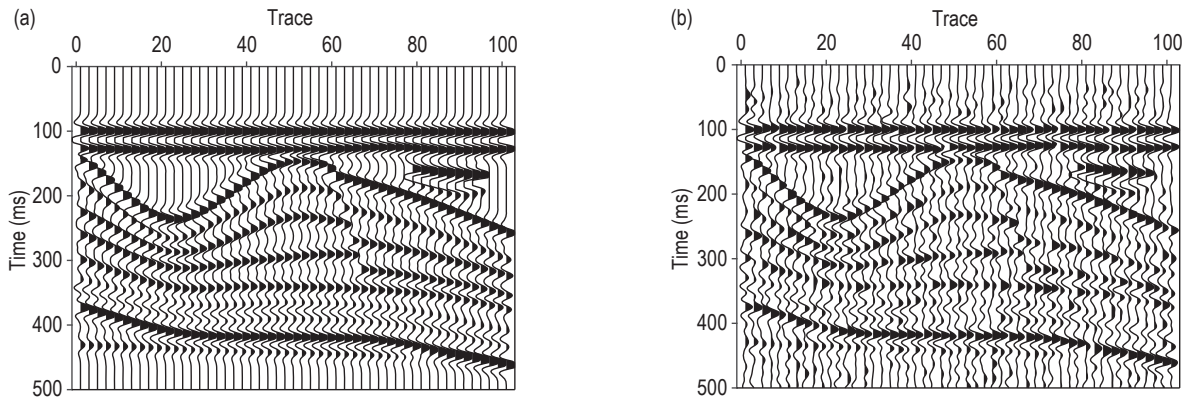
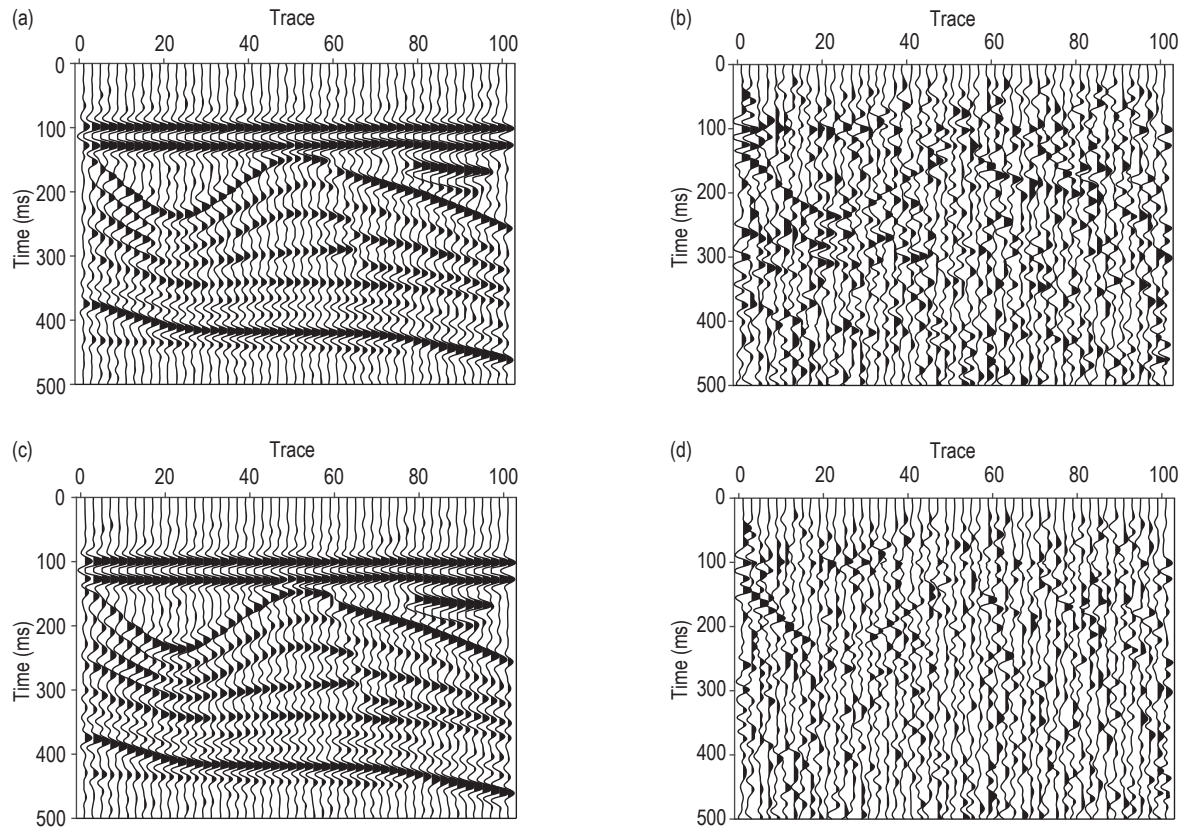


Fig. 5. Geological model (a) clean data, (b) noisy data.



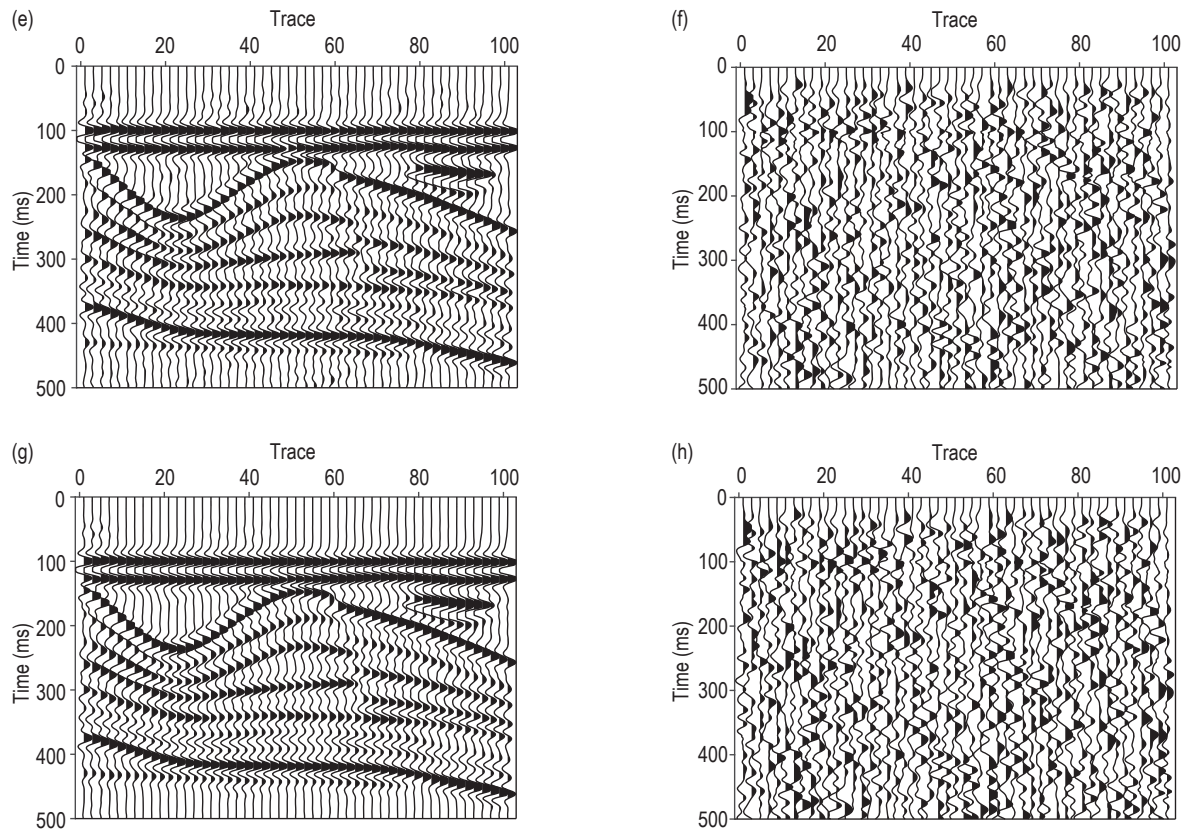


Fig. 6. Comparison of the three methods: (a) the denoised results by RNA (b) the removed noise by RNA (c) the denoised results by IRNA (d) the noise removed by IRNA (e) the denoised results by APF (f) the noise removed by APF (g) the denoised results by NSI (h) the noise removed by NSI.

Field data examples

The field data shown in Figure 7 are from an oil field in eastern China. For comparison, we use RNA and IRNA to process this data simultaneously. The RNA is implemented with the PF length of 7. For IRNA, the PF length in the time and space direction are 21 and 14, respectively ($mt = 10$ and $mx = 7$ in equation (3)); the trade-off parameter is 2. For NSI, the NPO's length in the time and space direction are 5 and 5, respectively ($M = 5$ and $N = 5$ in equation (8)); the trade-off parameter is 10. Figure 8 shows the denoised results and removed noise by the three methods. The three methods effectively suppress random noise when the events are approximately linear, and seismic data is quasi-stationary (the dip and amplitude of events are varying smoothly) (see Figures. 8 (a), (c), and (e). In the area of complex structure (such as faults), RNA and IRNA remove many effective signals (see Figure 8 (b), (d)). Compared with the two methods, the proposed method removes noise

and preserve signal effectively (see Figures 8 (e), (f)), especially for complex structure.

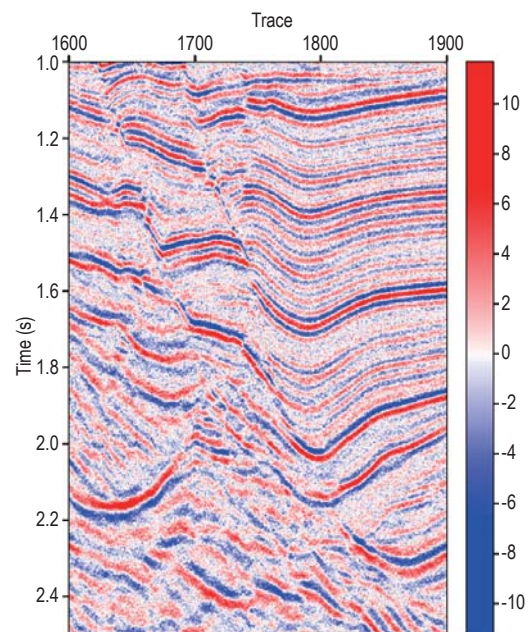


Fig. 7. Seismic field data.

Nonstationary signal inversion based on shaping regularization

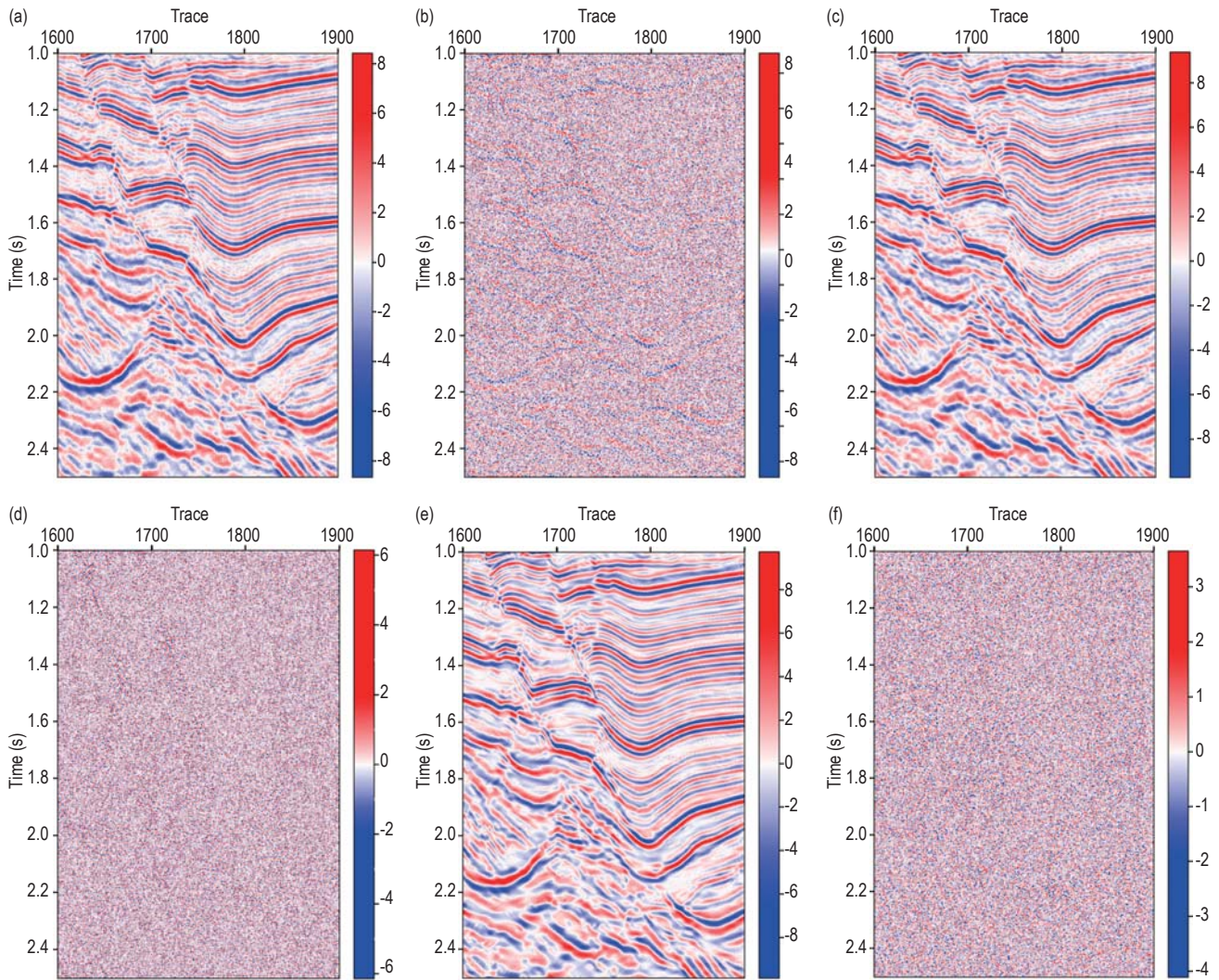


Fig. 8. Comparison of the three methods. (a) the denoised results by RNA, (b) the removed noise by RNA, (c) the denoised results by IRNA, (d) the noise removed by IRNA, (e) the denoised results by NSI, and (f) the noise removed by NSI.

Conclusions

We proposed a novel method for random noise attenuation using nonstationary signal inversion. In the method, the nonstationary signal inversion is taken as the denoising frame. The NPO calculated by shaping regularization is taken as the structural constraint in the inversion; thus, the effective signal can be directly inverted from the noisy seismic data. The experimental results showed that the denoising frame is a nonstationary signal inversion, which can overcome the model inconsistency before and after denoising, improving the signal-preserving ability. The NPO calculated by shaping regularization is varying spatiotemporally, describing the complex geological

structure. Therefore, the proposed method does not assume seismic data to be piecewise stationary and linear. Compared with RNA and IRNA, NSI removes noise and effectively preserves signals, especially for complex structures. Compared with APF, NSI has a more obvious denoising effect. The NPO length (M , N), smoothing radius, and trade-off parameter are the key parameters that affect the denoising effect of the method. The NPO length is related to the dip of events (Liu et al., 2012; Liu et al., 2014). The longer the NPO is, the more accurate the seismic signal structure can be described, but the higher the calculation cost will be. The larger the smoothing radius, the more obvious the denoising effect. Still, it will remove some structural details, resulting in poor signal-preserving performance. The trade-off parameter affects the performance of the method in

noise attenuation and signal preservation; thus, it needs to be determined by experiment. The application of synthetic seismic data and field data demonstrated that the proposed method performs better in suppressing random noise and preserving nonstationary signals. However, the proposed method converts the denoising problem into an inversion, improving the denoising effect and reducing the computational efficiency. Therefore, how to further improve computational efficiency will be the focus of future research.

Acknowledgements

*This research was financially supported by the CNPC Science Research and Technology Development Project (No. 2019A-3312), the CNPC major promotion project (No. 2018D-0813), the National Natural Science Foundation of China (No. 41874141) and the Project, “New Technology and Software Development for Comprehensive Identification and Evaluation of Cracks” of the Research Institute of Petroleum Exploration & Development-Northwest of CNPC (No. 2015B-3712). We also are grateful to our reviewers, Prof. Li Hui, Wang Yanchun, and Ma Jinfeng, for their feedback that assisted in substantially improving the presentation of this paper.

References

- Abma, R., and Claerbout, J., 1995, Lateral prediction for noise attenuation by t-x and f-x techniques: *Geophysics*, **60**(6), 1887–1896.
- Alan, R. M., and Panos, G. K., 1990, Efficient tau-p hyperbolic velocity filtering: *Geophysics*, **55**(5), 619–625.
- Bednar, J. B., 1983, Applications of median filtering to deconvolution, pulse estimation, and statistical editing of seismic data: *Geophysics*, **48**(12), 1598–1610.
- Canales, L., 1984, Random noise reduction: 54th Annual International Meeting, SEG, Expanded Abstracts, 525–527.
- Chase, M. K., 1992, Random noise reduction by FX prediction filtering: *Exploration Geophysics*, **23**, 51–56.
- Claerbout, J. F., 1992, Earth soundings analysis: Processing versus inversion: Blackwell Scientific Publications.
- Crawley, S., Clapp R., and Claerbout J. F., 1999, Interpolation with smoothly nonstationary prediction-error filters: 69th Annual International Meeting, SEG, Expanded Abstracts, 1154–1157.
- Fomel, S., 2007, Shaping regularization in geophysical-estimation problems: *Geophysics*, **72**(2), R29–R36.
- Fomel, S., 2009, Adaptive multiple subtraction using regularized nonstationary regression: *Geophysics*, **74**(1), V25–V33.
- Gholami, A., 2014, Non, convex compressed sensing with frequency mask for seismic data reconstruction and denoising. *Geophysical Prospecting*: **62**(6), 1389–1405.
- Gulunay, N., 1986, FXDECON and complex wiener prediction filter: 56th Annual International Meeting, SEG, Expanded Abstracts, 279–281.
- Jones, I. F., and Levy, S., 1987, Signal-to-noise ratio enhancement in multichannel seismic data via the Karhunen-Love transform: *Geophysical Prospecting*, **35**, 12–32.
- Liu, G. C., and Chen, X. H., 2013, Noncausal f-x-y regularized nonstationary prediction filtering for random noise attenuation on 3D seismic data: *Journal of Applied Geophysics*, **93**, 60–66.
- Liu, G. C., Chen, X. H., Du, J., et al., 2012, Random noise attenuation using f-x regularized nonstationary autoregression: *Geophysics*, **77**(2), V61–V69.
- Liu, Y., and Fomel, S., 2010, Trace Interpolation Beyond Aliasing Using Regularized Nonstationary Autoregression: 80th Annual International Meeting, SEG, Expanded Abstracts, 3662–3667.
- Liu, Y., Liu, N., and Liu, C., 2014, Adaptive prediction filtering in t-x-y domain for random noise attenuation using regularized nonstationary autoregression: *Geophysics*, **80**(1), V13–V21
- Liu, Z. P., Chen, X. H., and Li, J. Y., 2009, Noncausal spatial prediction filtering based on an ARMA model: *Applied Geophysics*, **6**(2), 122–128.
- Neelamani, R., Baumstein, A. I., Gillard, D. G., Hadidi, M. T., and Soroka, W. L., 2008, Coherent and random noise attenuation using the curvelet transform: *The Leading Edge*, **27**(2), 240–248.
- Rudin, L. I., Osher, S. and Fatemi, E., 1992, Nonlinear total variation based noise removal algorithms: *Physica D*, **60**(1–4), 259–268.
- Sacchi, M., and Kuehl, H., 2001, ARMA formulation of FX prediction error filters and projection filters: *Journal of Seismic Exploration*, **9**, 185–198.

Nonstationary signal inversion based on shaping regularization

- Soubaras, R., 1994, Signal-preserving random noise attenuation by the f-x projection: 64th Annual International Meeting, SEG, Expanded Abstracts, 1576–1579.
- Soubaras, R., 2000, 3D projection filtering for noise attenuation and interpolation: 70th Annual International Meeting, SEG, Expanded Abstracts, 2096–2099.
- Sun, Y., and Ronen, S., 1996, The pyramid transform and its application to signal/noise separation: Stanford Exploration Project Annual Report, **93**, 161–176.
- Wang, F., and Chen, S., 2019, Residual learning of deep convolutional neural network for seismic random noise attenuation: IEEE Geoscience and Remote Sensing Letters, **16**(8), 1314–1318.
- Yu, S., Cai, X., and Su, Y., 1989, Seismic signal enhancement by polynomial fitting: Applied Geophysics, **1**, 57–65.
- Yuan, S. Y., Wang, S. Y., and Li, G. F., 2012, Random noise reduction using Bayesian inversion: Journal of Geophysics and Engineering, **9**, 60–68.
- Zhang, R., and Ulrych T. J., 2003, Phasical wavelet frame denoising: Geophysics, **68**(1), 225–231.
- Zhao, Y. M., Li, G. F., Wang W., et al., 2017, Inversion-based data-driven time-space domain random noise attenuation method: Applied Geophysics, **14**(4), 543–550.
- Zhao, Y. X., Li, Y., and Yang, B. J., 2020, Denoising

of seismic data in desert environment based on a variational mode decomposition and a convolutional neural network: Geophysical Journal International, **221**(2), 1211–1225.

Yang Wuyang, Ph.D., senior technical expert of CNPC, graduated from Graduate School of the Chinese Academy of Geological Sciences in 2005, currently working in heterogeneous reservoir prediction, fractures modeling, and intelligent geophysical exploration.



Email: yangwuyang@petrochina.com.cn

Wang Wei (Communication author), a master's degree in geological resources and geological engineering from China University of Petroleum (Beijing) in 2018, currently working in the Institute of Geophysics, Northwest Branch of China Petroleum Exploration and Development Research Institute, mainly engaged in intelligent geophysical exploration, signal processing, and software development.



Email: wangwei_geophy@petrochina.com.cn